

INTERFACIAL STRUCTURES IN UPWARD HUGE WAVE FLOW AND ANNULAR FLOW REGIMES

K. SEKOGUCHI and M. TAKEISHI
Osaka University, Suita, Osaka 565, Japan

(Received 1 October 1988; in revised form 16 November 1988)

Abstract—The experimental results of time-spatial phase distributions are presented for vertical upward huge wave and annular flows. Two multi-integrated phase-sensing units were used to investigate the phase distributions, namely, the supermultiple-point-electrode probes (Super-PEP), for detecting time-varying cross-sectional phase distributions, and the supermultiple-ring-electrode probes (Super-REP), capable of observing the axial distributions of liquid lumps (e.g. liquid slugs, huge waves, disturbance waves and ephemeral large waves) and their behavior along a tube. A computer algorithm for determining the gas-liquid interface between the gas-core and a continuous liquid film or gas and liquid slugs is proposed, and some typical displays of three-dimensional interface structures are presented. The appearance of a huge wave and the disappearance of liquid slugs within a churn flow regime are pointed out based on the information of the interfacial structures.

Key Words: interfacial structure, huge wave, disturbance wave, liquid lump behavior, appearance frequency, existence limit

1. INTRODUCTION

A vast amount of observational work on gas-liquid two-phase flow has been done to examine spatial phase distributions or gas-liquid interfacial structures which are considered to be closely linked with the flow mechanisms. Phase distributions for bubble, slug and annular flows, except wispy annular flow, have been clarified to some extent to date. In froth and churn flows the interfaces are very rough, so usually there are considerable problems in specifying the profiles, especially for churn flow. The same difficulties have been encountered in wispy annular flow.

Recently, a specially designed phase-sensing device and a special electronic circuit system for data processing were developed and successfully employed to determine the interfacial structures in the disturbance wave regime of annular flow (Sekoguchi *et al.* 1985). This phase-sensing device was called supermultiple-point-electrode probes (Super-PEP) and consists of 24 clusters containing 409-point-electrode probes in a cross section, with which time-varying interfaces in the cross section can be detected and displayed through a computer.

The other type of phase-sensing device was newly developed and used simultaneously in combination with the Super-PEP for observing the behavior of liquid lumps, such as liquid slugs, huge waves, disturbance waves and ephemeral large waves, along a tube. This device contains 94 pairs of ring-shaped electrode probes located over the tube length of about 2.3 m and can provide the time-varying cross-sectional mean liquid holdup value at each probe (Sekoguchi *et al.* 1984, 1987). This device was named supermultiple-ring-electrode probes (Super-REP).

This paper reports the application of these phase-sensing systems for the determination of time-spatial phase distributions in the flow regimes of froth to annular flow. The churn flow regime lies within this range. Key words characterizing churn flow such as "unstable", "frothy", "disordered", "destruction of slug flow" and "oscillatory or alternating direction of motion of a liquid" can be found in the literature (Hewitt & Hall-Taylor 1970; Collier 1972; Taitel *et al.* 1980; Delhaye 1981; Whalley 1987). These words commonly suggest that churn flow has an extremely complicated gas-liquid interface, the structure of which remains obscure; i.e. the presence of liquid slugs is not definite although there is a sketch of a churn flow pattern in which a liquid lump, just like a liquid slug, axially-separating gas phase is depicted. The information on the interface obtained in the present experiment is used to resolve such problems.

In order to examine the interface between the gas-core and a continuous liquid film or gas and liquid slugs, a computer algorithm was developed. Typical computer graphics of interfaces

processed by the algorithm are demonstrated for two flow regimes: (1) the huge wave flow regime, characterized by the existence of a huge wave or large-scale wave with a wide range of transit velocities (Sekoguchi *et al.* 1984); and (2) the disturbance wave regime of annular flow.

A method for discrimination between liquid slugs, huge waves, disturbance waves and ephemeral large waves is described. The existence limits for liquid slugs, huge waves and disturbance waves are proposed using the experimental results on the appearance frequencies of these liquid lumps.

2. EXPERIMENTAL

A schematic diagram of the experimental setup is shown in figure 1. The test section was an acrylic resin tube of 25.8 mm i.d. The tube was positioned exactly vertical. Metered streams of air and water were led to a mixer where the water (or air) was injected into the air (or water) flowing inside the tube through injection holes drilled around the tube periphery.

Two instrument systems, consisting of different types of multi-integrated phase-sensing units, their electronic interfaces and computers, were used for determining time-spatial phase distributions. One of the phase-sensing units was the Super-PEP (comprising 409 electrical needle probes arranged on a tube cross section), with which time-varying cross-sectional phase distributions were detected. The spatial resolution of this measuring system evidently depends upon the spacing between the probes and the sampling frequency. Taking account of the order of magnitude of the film thickness and disturbance wave height in annular flow, available from the literature, the minimum radial spacing selected was $50\ \mu\text{m}$ over a distance from the wall to $250\ \mu\text{m}$, and the remaining spacings were successively taken as 0.1, 0.1, 0.15, 0.3, 0.35, 0.4, 0.6, 0.9, 1.0, 1.5, 1.9, 2.5 and 3.2 mm. The circumferential spacings were varied from 3.4 mm near the wall to 0.84 mm near the center. The details of this unit and its electronic system are given elsewhere (Sekoguchi *et al.* 1985).

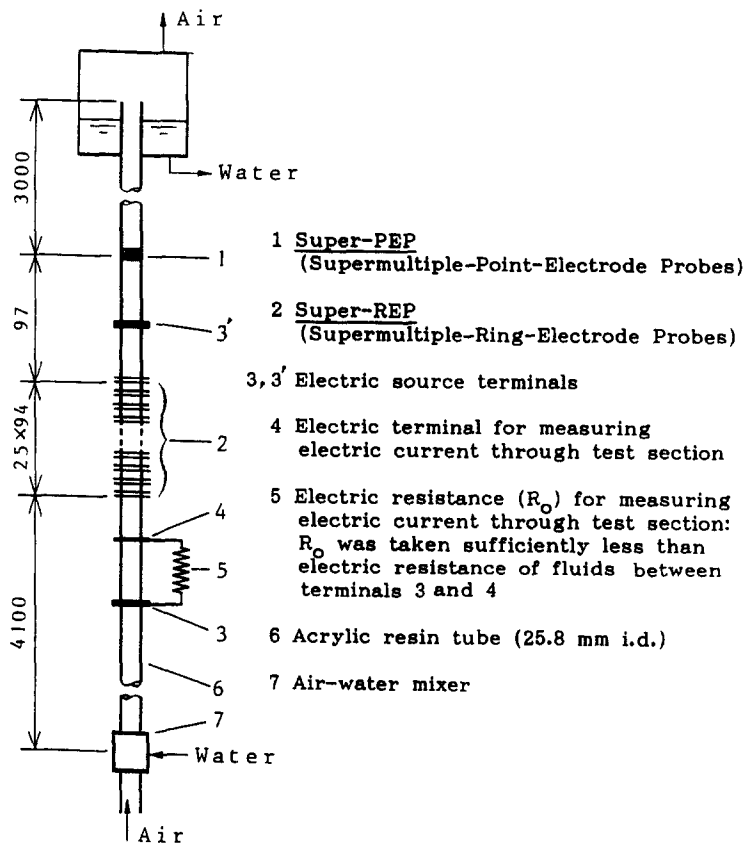


Figure 1. Schematic diagram of the experimental setup.

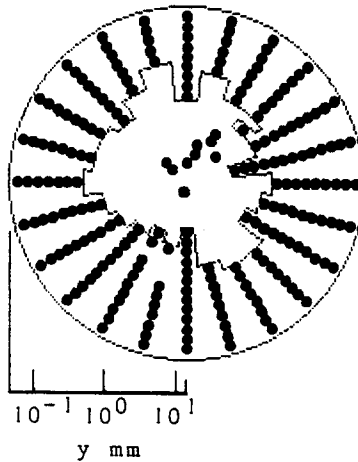


Figure 2. Explanatory example of the distribution of the liquid-sensing probes for the algorithm for tracing the interface. ●, Liquid-sensing probe.

The other unit was the Super-REP (comprising 94 pairs of ring-type electrodes arranged axially with a spacing of 25 mm over the length of 2.325 m), as shown in figure 1. Individual ring-electrode probes provide time-varying values of the tube cross-sectional mean liquid holdup along the tube, which are measured from both the variation in the electrical resistivity of the liquid between each pair of ring-electrodes and the variation in the electric current through the test section (Sekoguchi *et al.* 1983).

The Super-PEP was mounted 97 mm downstream of the upper end of the Super-REP, and these two multi-integrated phase-sensing units were used simultaneously. Sampling frequencies were 1 kHz and 400 Hz, and data memory capacities were 1.2 and 2 M 8-bit words for the Super-PEP and Super-REP, respectively. The computers employed in this study were 16-bit, NEC PC9801VX2 and TEAC PS9000 (HP216).

The flow conditions tested were as follows:

pressure	0.2 MPa
temperature	20–22°C
superficial air velocities	1–30 m/s
superficial water velocities	0.1–0.7 m/s.

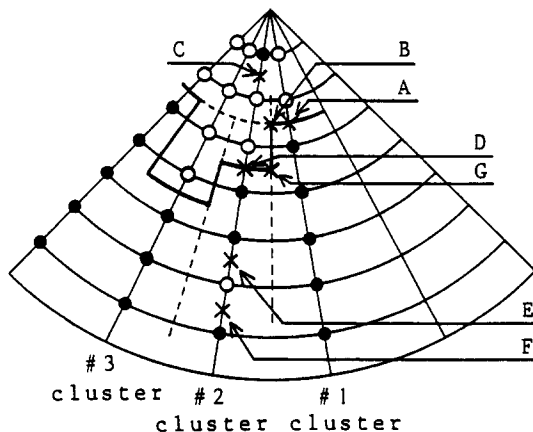


Figure 3. Procedure to determine the interface between the gas-core and the annular liquid. ----, Traced interface; ●, liquid-sensing probe; ○, gas-sensing probe.

3. ALGORITHM FOR DETERMINING THE GAS-LIQUID INTERFACE IN A LIQUID FILM

The Super-PEP discriminates between gas or liquid at 409 locations in a tube cross section and supplies lateral discrete information on the phases which are attributed to various gas-liquid interfacial structures formed from bubbles, large liquid drops or waves. The figure of 409 phase-sensing points may be insufficient to enable us to determine detailed interfaces such as those of small bubbles and entrained droplets. This study, however, chiefly aims to deal with the gas slug profile and the interfaces between the gas-core and the continuous liquid phase except those of relatively smaller bubbles and liquid droplets.

Figure 2 shows an example of the distribution of probes which detect the liquid phase across the tube for the flow condition with superficial gas velocity $j_G = 7$ m/s and superficial liquid velocity $j_L = 0.3$ m/s. Obviously there are two different situations for these liquid-sensing probes; i.e. a liquid-sensing probe is either completely surrounded by gas-phase-sensing probes or neighbor to at least one other liquid-sensing probe. The former is considered to indicate a liquid mass isolated from the annular liquid whose interface is required. Therefore, all the signals from the isolated probes are ignored, whereas those from the remaining probes are used to determine the interface.

The procedure employed for this determination through a computer is explained below using the example shown in figure 3:

- (1) Find a pair of neighboring probes, detecting gas and liquid phases, on the first arbitrarily selected cluster.
- (2) Take the position of the interface as halfway between these probes, point "A".
- (3) Locate a point "B" which lies on a circle of the same radius as point "A" and between the first and second clusters.
- (4) Find points "C", "D", "E" and "F", the next possible interface on the second cluster. In such a case the interface is traced in the counterclockwise direction, and the point to be selected among "C" through "F" is the one nearest to "B". Thus, the interface can be drawn from "B" through "G" to "D".
- (5) Apply the same procedure to all the remaining clusters and determine a closed interface.
- (6) When two or more interfaces are obtained, the one with the greatest peripheral length is selected.

4. RESULTS AND DISCUSSION

4.1. Gas-liquid interfacial structure at the incipient stage of the gas-core formation

Figures 4(a-c) show representative gas-liquid interfaces in a huge wave flow regime ($j_G = 5$ and 7 m/s for $j_L = 0.3$ m/s; and $j_G = 5$ m/s for $j_L = 0.1$ m/s) processed by means of the algorithm described in section 3. This display takes the form whereby a cross section of the tube is converted into a semicircular section to make it easier to see three-dimensional interfaces (wave height, y ; angular position of the probe cluster, ϕ ; time, t). Liquid lumps of various size appear in the figure (liquid slugs, huge waves and ephemeral large waves are denoted by S, H and E, respectively), which were determined by the procedure described here and in the following sections.

Figures 5(a,b) are the consecutive cross-sectional graphics for the liquid lumps # 5 ($\textcircled{A}-\textcircled{A}'$) and # 6 ($\textcircled{B}-\textcircled{B}'$), as shown in figure 4(a). The time interval for the illustrations is 1 ms. It is clearly seen that the gas-core is formed in liquid lump # 5 but not in # 6. In this case, the former is a huge wave and the latter is a liquid slug. Liquid lumps # 1 and # 4 in figure 4(a) are also huge waves. Huge waves are greater not only in dimension but have higher transit velocities than other types of wave (i.e. disturbance waves and ephemeral large waves). On the basis of these features, huge waves can be distinguished from disturbance waves; details are given in section 4.2.

The separation distance between liquid lumps # 5 and # 6 is about 2 m, which can be measured easily on the wave behavior map, as shown later in figure 6. The total length of the test section is about 10 m. Therefore, it is relatively longer than the separation distance. This fact suggests that huge waves and liquid slugs can simultaneously coexist in the tube.

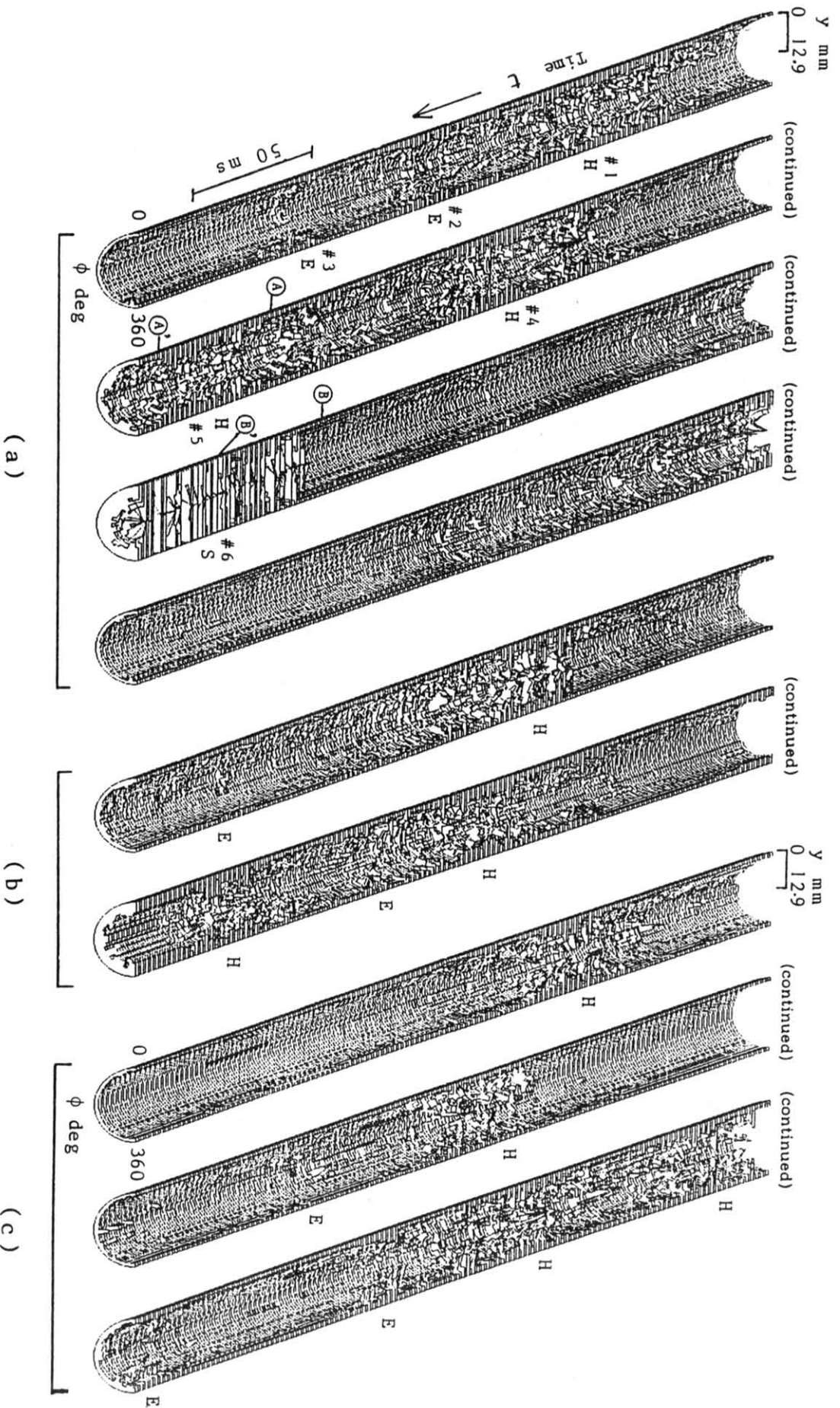


Figure 4. Three-dimensional contours of an interface developed on a semicircular cross section of the tube: (a) $J_G = 5$ m/s, $J_L = 0.3$ m/s; (b) $J_G = 7$ m/s, $J_L = 0.3$ m/s; (c) $J_G = 5$ m/s, $J_L = 0.1$ m/s.

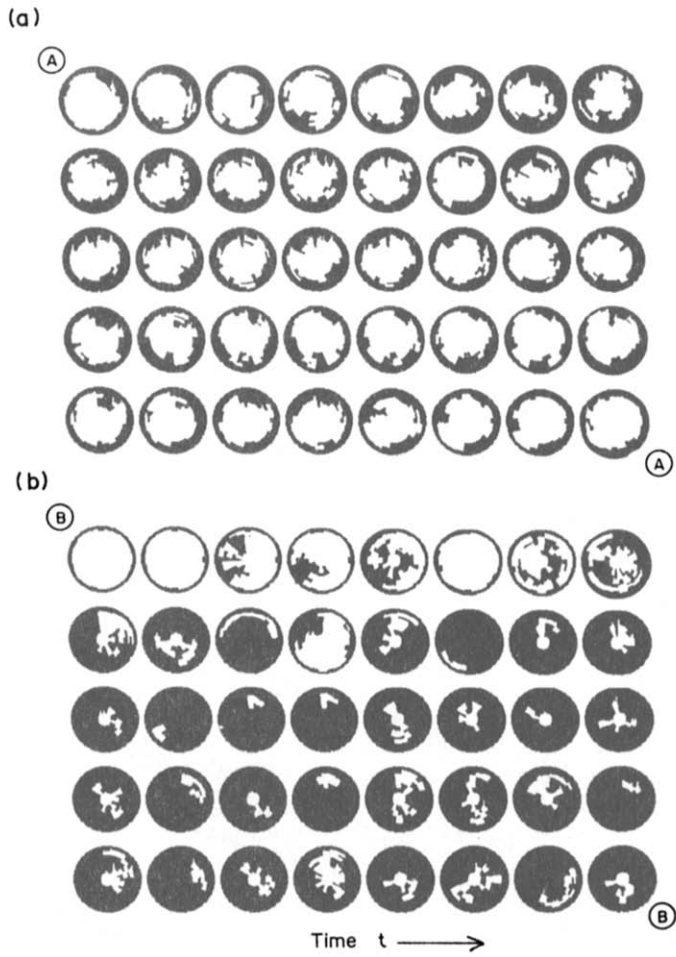


Figure 5. Consecutive cross-sectional graphics for the liquid lumps #5 ((A)–(A')) and #6 ((B)–(B')) shown in figure 4(a). The time interval for the illustrations is 1 ms.

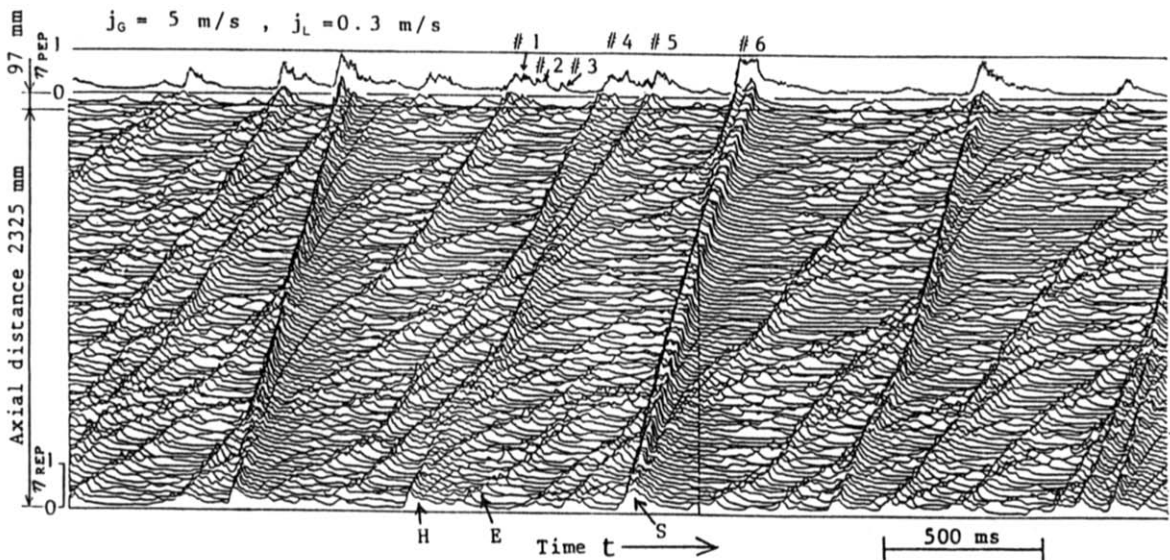


Figure 6. Wave behavior map drawn from the mean liquid holdup signals, η_{REP} , detected with Super-REP, and the mean liquid holdup, η_{PEP} , measured with Super-PEP ($j_G = 5 \text{ m/s}$, $j_L = 0.3 \text{ m/s}$).

Further examples of interfacial structure are shown in figures 4(b, c). No liquid slug is observed under these flow conditions: namely, the gas-cores are completely formed. It should be noted that according to the flow pattern map of Hewitt & Roberts (1969), the case in figure 4(b) belongs to annular flow and that in figure 4(c) to churn flow; further discussion of this is presented in section 4.3.

It is quite difficult to discriminate between liquid slugs and huge waves when normal observational techniques, e.g. still photography, high-speed cinematography (Hall-Taylor *et al.* 1963) or X-ray tomography (Narabayashi *et al.* 1984), are employed. However, it is very simple and definite if information on the consecutive cross-sectional phase distribution is available. Such a method was adopted for the present study.

Figure 6 shows the wave behavior map for the flow condition with $j_G = 5$ m/s and $j_L = 0.3$ m/s, in which time-varying signals of the cross-sectional mean liquid holdup (η_{REP}) are recorded along the tube. When the cross-sectional mean liquid holdup is measured by the ring-electrode probe, the nonuniform axial distribution of the liquid phase causes nonuniformity of the electrical current density inside the liquid phase, and hence some inaccuracy in the measurement because the liquid holdup is evaluated using a relation based on an electrical current of uniform density. A more reliable value of the liquid holdup, however, can be estimated from the data obtained by the Super-PEP (η_{PEP}). For comparison, such a result is included in the figure.

The liquid lumps numbered #1 through #6 are the same as those shown in figure 4(a). In general a liquid slug moves with a nearly constant velocity so that its trace is almost linear, whereas a huge wave follows a zigzag path and has varying velocity. Many ephemeral large waves appear whose traces can be followed without difficulty, although these waves are frequently absorbed by liquid slugs and huge waves and also discharged from the rear of such liquid lumps. The figure also indicates that it is possible for relatively smaller waves originating from the rear of liquid slugs to develop into huge waves.

4.2. Gas-liquid interfacial structure of waves in an annular liquid film

Figure 7 shows another example of three-dimensional interfaces in huge wave and annular flow regimes expressed in cartesian coordinates, which were treated with a smoothing operation (the average of five data points was taken—a central point and its four nearest neighbors, consisting of two in an angular position and also two in time). It can be seen that the principal undulation of the interface is brought into bold relief after the smoothing operation.

The classification of the liquid lumps in figure 7 was made by taking account of their axial movements and velocities on wave behavior maps, as expressed in figure 6. In addition to the visual examination of individual waves, the following criteria regarding wave velocity were introduced for the classification:

- (a) First, the velocity of the disturbance wave u_{Dex} is experimentally determined by the time-lapse method, in which a pair of cross-sectional mean holdups are used (Sekoguchi *et al.* 1984). Usually a disturbance wave has a nearly constant velocity along the tube in the region typical of disturbance waves, and the mean velocity changes linearly with increasing superficial gas velocity at a constant liquid flow rate on a double logarithmic chart. The relation between u_{Dex} and j_G is extrapolated towards the flow region with decreasing values of j_G , where u_{Dex} fluctuates along the tube as would be imagined from figure 8. When considering the experimental results for the standard deviation of the disturbance wave velocity (Takeishi *et al.* 1987), it is assumed, therefore, that the velocity of the disturbance wave lies within 20% of the extrapolated line of u_{Dex} vs j_G .
- (b) Ephemeral large waves obviously have lower velocities than disturbance waves (cf. figure 8), hence all waves with velocities $< 0.8 u_{\text{Dex}}$ are assumed to be ephemeral large waves.
- (c) The remaining waves, except for disturbance waves and ephemeral large waves, are regarded as huge waves; i.e. the velocity of a huge wave is assumed to be $> 1.2 u_{\text{Dex}}$.

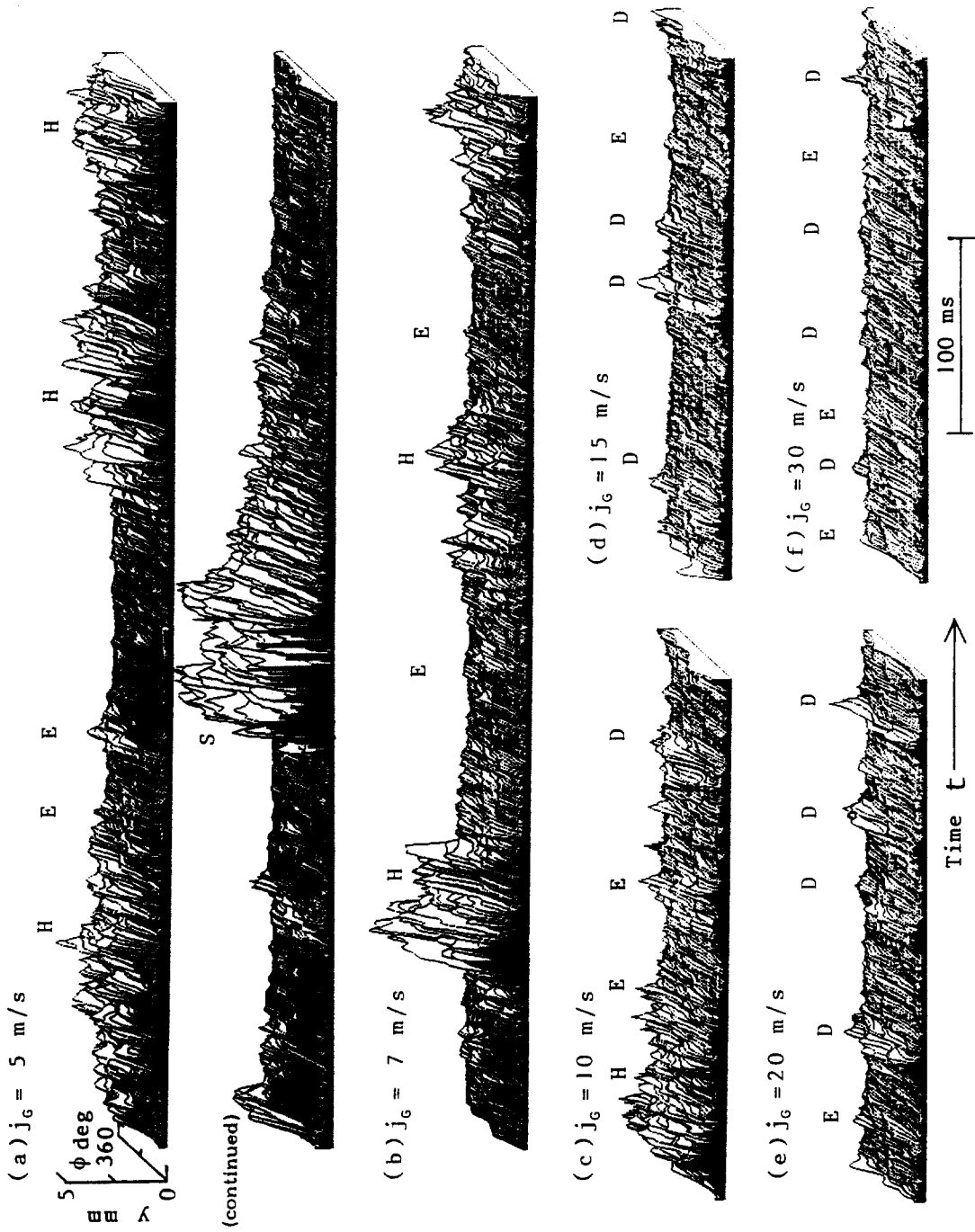


Figure 7. Three-dimensional contours of an interface developed in cartesian coordinates ($j_i = 0.3 \text{ m/s}$).

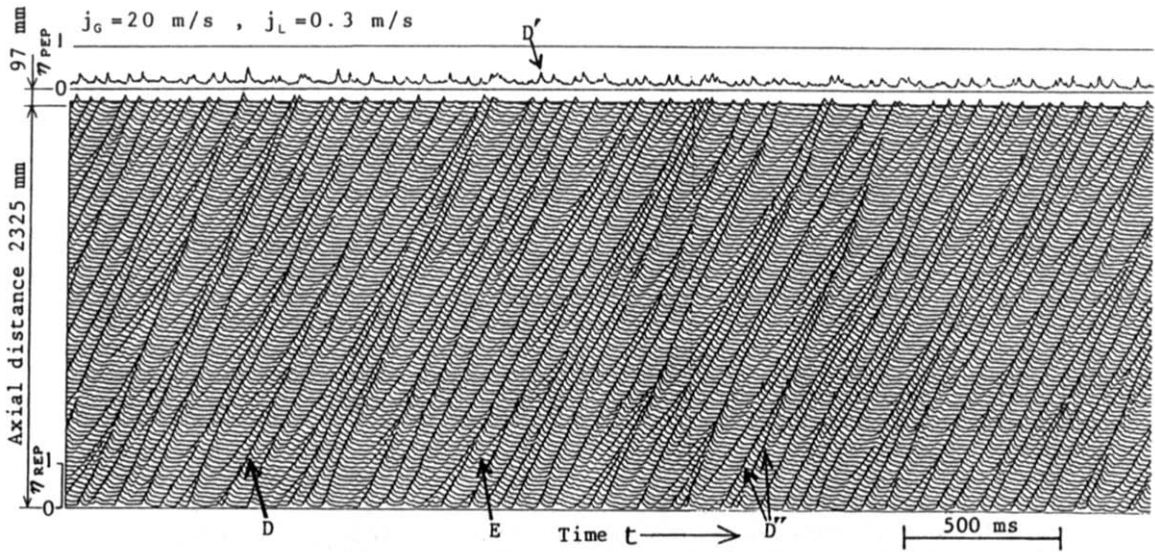


Figure 8. Wave behavior map drawn from the mean liquid holdup signals, η_{REP} , detected with Super-REP, and the mean liquid holdup, η_{PEP} , measured with Super-PEP ($j_G = 20$ m/s, $j_L = 0.3$ m/s).

From scrutiny of figure 7, we summarize some interesting aspects of the results as follows:

- (1) In spite of the large difference in volume between liquid slugs and huge waves, their residence times are of comparable orders of magnitude [cf. figure 7(a)].
- (2) The volumes of huge waves differ greatly even for the same flow condition [cf. figure 7(b)].
- (3) The volume and residence times of huge waves are essentially large compared with those of disturbance waves [cf. figure 7(c)].
- (4) Ephemeral large waves are capable of possessing the same dimensions as disturbance waves [cf. figures 7(c-f)].

Figure 8 is a wave behavior map for annular flow. It is evident that the disturbance wave absorbs and discharges ephemeral waves and the velocity of the disturbance wave is affected accordingly by the absorption and discharge of ephemeral waves. As can be seen from the traces labelled D' and D'' , there is a possibility that the disturbance wave is newly produced (D') or that two disturbance waves coalesce into one new disturbance wave (D'').

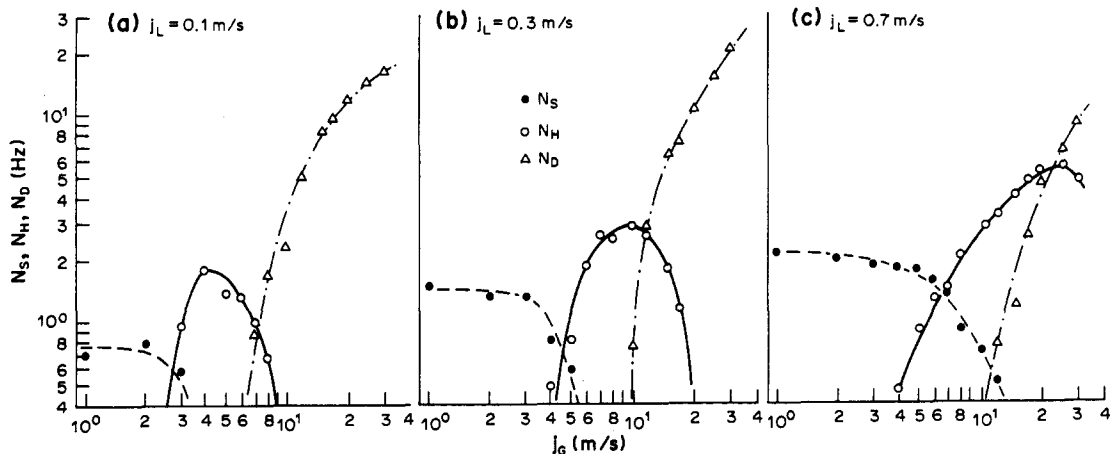


Figure 9. Appearance frequencies of liquid lumps (N_S , N_H and N_D represent liquid slugs, huge waves and disturbance waves, respectively).

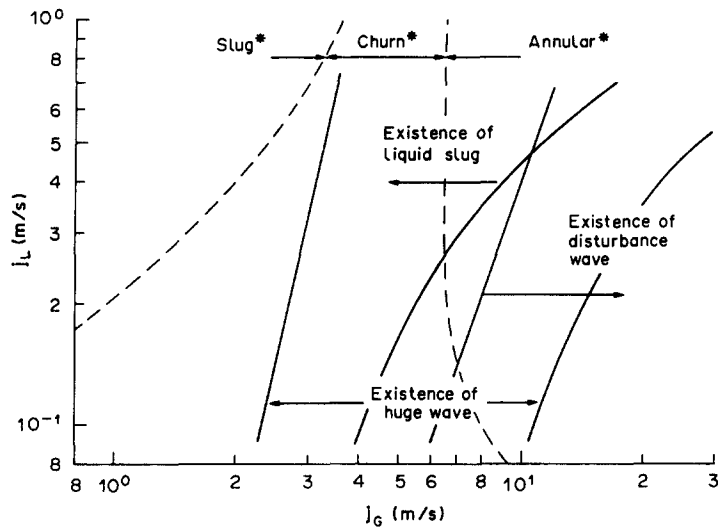


Figure 10. Existence limits for liquid slugs, huge waves and disturbance waves. ---, Boundaries for flow patterns (Slug*, Churn* and Annular*) proposed by Hewitt & Roberts (1969).

4.3. Appearance frequencies of liquid slugs, huge waves and disturbance waves

Figures 9(a-c) show the appearance frequencies of liquid slugs, huge waves and disturbance waves, whose discriminating features have been described in the previous sections. The appearance or disappearance of these liquid lumps strongly depends upon the flow rates of both phases, but there are some common features between them. Considering figure 9(b), for example, the appearance frequency of the liquid slug N_S is almost independent of j_G for $j_G < 3$ m/s, but decreases rapidly with increasing j_G beyond 3 m/s and diminishes at $j_G = 7$ m/s. A huge wave appears around $j_G = 3$ m/s, and its appearance frequency N_H increases with j_G ; it begins to decrease at $j_G = 10$ m/s, becoming negligibly small at $j_G = 20$ m/s. A disturbance wave begins to appear at $j_G = 8$ m/s and increases its frequency N_D monotonously to the upper limit of the values measured for j_G .

From such appearance frequency data, the existence limits for individual liquid lumps can be drawn. In figure 10, these limits for huge waves and disturbance waves were determined so as to satisfy the following relations:

$$N_H = 0.1N_S \text{ to } 0.1N_D \text{ for huge waves;}$$

$$N_D = 0.1N_H \text{ for disturbance waves.}$$

The existence limit for liquid slugs was determined as $N_S = 0$. For comparison a flow pattern map (Hewitt & Roberts 1969) is overlapped in the figure. It can be seen that huge waves occur within both the churn and annular flow regimes, liquid slugs appear partly in the annular flow regime while partly disappearing in the churn flow regime and disturbance waves initiate roughly within the annular flow regime.

5. CONCLUSIONS

This study examined the time-spatial distribution of gas and liquid phases. The results obtained are summarized as follows:

- (1) The interfacial structure in churn flow was clarified.
- (2) There are two types of flow in the churn flow regime: one has a gas-core and the other has liquid slugs.
- (3) Interfacial features and the longitudinal behavior of huge waves were outlined, and hence the flow regime characterized by the presence of huge waves was clarified.
- (4) A method to discriminate between huge waves, disturbance waves and ephemeral large waves was proposed, with which two zones exhibiting the coexistence of liquid slugs and huge waves and huge waves and disturbance waves were found.

Acknowledgements—The authors wish to express their appreciation to Messrs K. Mori, M. Sugata, H. Fukuda and K. Kawanishi whose enthusiastic efforts have aided the research.

REFERENCES

- COLLIER, J. G. 1972 *Convective Boiling and Condensation*. McGraw-Hill, New York.
- DELHAYE, J. M. 1981 *Two-phase Flow Patterns, Two-phase Flow and Heat Transfer in the Power and Process Industries*, pp. 1–39. Hemisphere, Washington, D.C.
- HALL-TAYLOR, N., HEWITT, G. F. & LACEY, P. M. C. 1963 The motion and frequency of large disturbance waves in annular two-phase flow of air–water mixtures. *Chem. Engng Sci.* **18**, 537–552.
- HEWITT, G. F. & HALL-TAYLOR, N. S. 1970 *Annular Two-phase Flow*. Pergamon Press, Oxford.
- HEWITT, G. F. & ROBERTS, D. N. 1969 Studies of two-phase flow patterns by simultaneous X-ray and flush photography. Report AERE-M2159.
- NARABAYASHI, T., TOBIMATSU, T., NAGASAKA, H. & KAGAWA, T. 1984 Scanning X-ray void fraction meter. In *Proceedings of IUTAM-Symposium; Measuring Techniques in Gas–Liquid Two-phase Flows*, pp. 259–280. Springer, Berlin.
- SEKOGUCHI, K., TAKEISHI, M., HIRONAGA, K. & NISHIURA, T. 1984 Velocity measurement with electrical double-sensing devices in two-phase flow. In *Proceedings of IUTAM-Symposium; Measuring Techniques in Gas–Liquid Two-phase Flows*, pp. 455–477. Springer, Berlin.
- SEKOGUCHI, K., TAKEISHI, M. & ISHIMATSU, T. 1985 Interfacial structure in vertical upward annular flow. *PhysicoChem. Hydrodynam.* **6**, 239–255.
- SEKOGUCHI, K., TAKEISHI, M., COGNET, G., ISHIMATSU, T. & YAHIRO, K. 1987 Patterns of liquid lump behaviors in upward gas–liquid two-phase flow. *Trans. Jap. Soc. mech. Engrs* **53**, 2807–2813. In Japanese.
- TAITEL, Y., BARNEA, D. & DUKLER, A. E. 1980 Modeling flow pattern transitions for steady upward gas–liquid flow in vertical tubes. *AIChE JI* **26**, 345.
- TAKEISHI, M., SEKOGUCHI, K., SHIMIZU, H. & NAKASATOMI, M. 1987 Velocity of liquid lumps in vertical upward gas–liquid two-phase flow. *Trans. Jap. Soc. mech. Engrs* **53**, 2800–2806. In Japanese.
- WHALLEY, P. B. 1987 *Boiling, Condensation and Gas–Liquid Flow*. Clarendon Press, Oxford.